Polymer Chemistry

PAPER

View Article Online
View Journal | View Issue

Cite this: *Polym. Chem.*, 2014, **5**, 2747

Unimolecular micelles composed of inner coil-like blocks and outer rod-like blocks crafted by combination of living polymerization with click chemistry†

Xinchang Pang,[a] Chaowei Feng,[a] Hui Xu,[ab] Wei Han,[a] Xukai Xin,[a] Haiping Xia,[b] Feng Qiu[c] and Zhiqun Lin*[a]

Received 28th November 2013
Accepted 23rd December 2013

DOI: 10.1039/c3py01657a

www.rsc.org/polymers

A new class of star-shaped coil–rod diblock copolymer polystyrene-*block*-poly(3-hexylthiophene) (PS-*b*-P3HT) with well-defined structures and the ratio of coil to rod blocks were synthesized by a combination of atom transfer radical polymerization, the Grignard metathesis method, and click reaction. The star-shaped PS-*b*-P3HT diblock copolymers covalently connected to a β-cyclodextrin (β-CD) core were composed of 21-arm coil-like PS inner blocks and rod-like conjugated polymer P3HT outer blocks with narrow molecular weight distribution. The intermediate and final products were systematically characterized and confirmed by gel permeation chromatography (GPC), ^{1}H nuclear magnetic resonance (^{1}H-NMR), and Fourier transfer infrared (FTIR) spectroscopy. The optical properties of star-shaped PS-*b*-P3HT were examined by UV-Vis absorption and photoluminescence (PL) measurements. In comparison to the linear P3HT, due to their compact structure and the introduction of PS blocks, the optical properties of 21-arm, star-shaped PS-*b*-P3HT were altered. The star-shaped PS-*b*-P3HT formed *unimolecular* micelles in good solvent as revealed by dynamic light scattering (DLS) and atomic force microscopy (AFM) studies.

Introduction

Star-shaped polymers consisting of more than three linear dissimilar or identical polymer chains of approximately equal lengths covalently joined to a core possess the simplest structure with numerous possible branched topologies.[1–4] Due to their compact structure, globular shape, and high concentration of terminal functional groups, star-shaped polymers exhibit high solubility in common solvents, low viscosity, and modified thermal properties as compared to linear analogues.[5–8] In comparison to linear polymers of a similar molecular weight, star-shaped polymers possess most of the properties of high molecular weight with low solution viscosity for a variety of applications, such as melt strength improvers, support for industrial catalysts, coatings, additives, drug and gene delivery, and supramolecular science.[1,9–13]

With development of controlled/living radical polymerization, especially atom transfer radical polymerization (ATRP) and reversible addition–fragmentation chain-transfer (RAFT) polymerization,[2,14–16] star-shaped polymers have been extensively synthesized.[17–23] Synthesis of star-shaped polymers can be categorized into two broad approaches, namely, (i) the arm-first method and (ii) the core-first method.[17–24] In the arm-first approach, the linear arms are prepared first, followed by connecting the arms to the core. The connection of arms is achieved by using either a difunctional monomer or a multifunctional terminating agent. When a difunctional monomer was used as a cross-linking agent to prepare star-shaped polymers, the number of arms in these star-shaped polymers cannot be precisely controlled.[25] When star-shaped polymers are synthesized by grafting onto a core having multifunctional terminating groups, the main problem is the nonselective and slow reaction between the linear polymer arm end and the multifunctional coupling agent.[2] In stark contrast, in the core-first method, star-shaped polymers are prepared utilizing a multifunctional initiator (the core) to initiate the growth of arms by the monomer addition. It has been successfully implemented to yield well-defined stars with a discrete number of arms.[2,24–26]

Among a variety of conjugated polymers, regioregular poly(3-hexylthiopene) (P3HT) is one of the most heavily studied organic semiconductors due to its good solubility, chemical

[a]*School of Materials Science and Engineering, Georgia Institute of Technology, Atlanta, GA 30332, USA. E-mail: zhiqun.lin@mse.gatech.edu; Fax: +1-404-385-3734; Tel: +1-404-385-4404*

[b]*State Key Laboratory of Physical Chemistry of Solid Surfaces and Department of Chemistry, College of Chemistry and Chemical Engineering, Xiamen University, Xiamen 361005, China*

[c]*Key laboratory of computational physical sciences and Department of Macromolecular Science, Fudan University, Shanghai 200433, China*

† Electronic supplementary information (ESI) available. See DOI: 10.1039/c3py01657a

stability, and excellent electronic properties.[27–33] The quasi-living Grignard metathesis (GRIM) polymerization technique[34,35] in conjunction with other living polymerization techniques such as ATRP,[36,37] ionic polymerization,[38–42] and ring-opening metathesis polymerization (ROMP)[43] allows the preparation of a diverse set of P3HT-based linear block copolymers. Thermodynamically, they are self-assembled into controllable architectures on a tens of nm length scale,[44–47] providing optimized morphologies for charge generation and transport.[48,49] To the best of our knowledge, due to the restricted functional groups on P3HT synthesized by GRIM, limited work has been performed on the preparation of P3HT-based multi-arm, star-shaped block copolymers with well-defined molecular structures.[50–52]

ATRP is a particularly attractive controlled/living radical polymerization technique for synthesis of chain-end functionalized polymers.[2,53] Polymers produced by ATRP retain terminal halogen atoms that can be subsequently converted into various desired functional chain-end groups through appropriate transformations, especially nucleophilic substitutions. On the other hand, owing to their quantitative yields, high specificity, and near-perfect fidelity regardless of most functional groups, click reactions termed by Sharpless *et al.*[54] have been widely used in polymer chemistry[2,55,56] during the past few years. Thus, it is very promising to judiciously combine ATRP with click reaction to yield functional block copolymers with complex architectures.

Herein, we report a facile strategy to craft a series of novel 21-arm, star-shaped coil–rod diblock copolymers composed of coil-shaped polystyrene (PS) inner blocks and rod-shaped P3HT outer blocks (*i.e.*, star-shaped PS-*b*-P3HT) based on β-cyclodextrin (β-CD) with well-defined molecular structures, molecular weights, and the fraction of different blocks *via* a combination of ATRP, quasi-living GRIM, and click reaction. β-CD is a cyclic oligosaccharide consisting of seven glucose units linked by α-1,4-glucosidic bonds. It possesses 21 hydroxyl groups that enable the synthesis of a star-shaped macroinitiator with 21 initiation sites to yield 21-arm, star-shaped block copolymers.[57–59] The optical properties of star-shaped coil–rod PS-*b*-P3HT were studied by UV-Vis absorption and photoluminescence (PL) measurements. Due to their compact structure, star-shaped PS-*b*-P3HT formed unimolecular micelles as revealed by atomic force microscopy (AFM), dynamic light scattering (DLS) and transmission electron microscopy (TEM) studies. This simple yet robust synthetic strategy opens up new ways to produce a large variety of multi-arm, star-shaped coli-rod block copolymers, and to explore the fundamental structure (*i.e.*, star-shaped architecture and the coil–rod conformation) and property relationship of functional star-shaped block copolymers for potential use in optoelectronics, biosensors, *etc.*[60–62]

Experimental section

Materials

2-Bromoisobutyryl bromide (98%), anhydrous 1-methyl-2-pyrrolidinone (99.5%), *N*,*N*,*N*′,*N*″,*N*″-pentamethyldiethylenetriamine (PMDETA, 99%), 2,2′-bipyridyl (bpy, >99%), sodium azide (≥99.5%), 2,5-dibromo-3-hexyl-thiophene (97%), *tert*-butylmagnesium chloride (2.0 M solution in diethyl ether), ethynylmagnesium bromide (0.5 M solution in tetrahydrofuran), [1,3-bis(diphenylphosphino)propane] dichloronickel(II), and β-cyclodextrin (β-CD, Sigma-Aldrich) were purchased from Sigma-Aldrich and used as received. CuBr (98%, Sigma-Aldrich) was purified according to our previous work.[8] Styrene (>99.5%, Sigma-Aldrich) was washed with 10% NaOH aqueous solution and water successively, dried over anhydrous $MgSO_4$, and further dried over CaH_2 and distilled under reduced pressure. All other reagents were purified by common purification procedures.

Characterization

Molecular weight and polydispersity index (PDI) of all polymers were measured by GPC, equipped with a G1362A refractive detector, a G1314A variable wavelength detector, and an Agilent1100 with a G1310A pump. THF was used as eluent at 35 °C at 1.0 mL min^{-1}. Two 5 μm LP gel mixed bed columns (molecular range: 200 to 3×10^6 g mol^{-1}) and one 5 μm LP gel column (500 Å, molecular range: 500 to 2×10^4 g mol^{-1}) were calibrated with PS standard samples. ^{1}H-NMR characterization was carried out by Varian VXR-400 spectroscopy, in which $CDCl_3$ was used as the solvent. FTIR spectra were recorded using a Magna-550 Fourier transform infrared spectrometer. Morphologies of 21-arm, star-shaped PS-*b*-P3HT unimolecular micelles were examined by atomic force microscopy (AFM; Dimension 3000) with the tapping mode at a 2 Hz scanning rate. AFM samples were prepared by spin-coating 0.1 mg mL^{-1} chloroform solution on a Si substrate at 2000 rpm (Headway PWM32 spin coater under ambient conditions). Each sample was imaged at more than five locations to ensure the reproducibility of features observed. The size and morphology of samples were examined by TEM (JEOL 100CX). TEM samples of star-shaped polymers were prepared by applying a drop of star-shaped polymer dichloromethane solution (1 mg mL^{-1}) onto a carbon-coated copper TEM grid (300 mesh) and allowing dichloromethane to evaporate under ambient conditions. Finally, the TEM grid was exposed to ruthenium tetraoxide (RuO_4) with which the PS and P3HT blocks were stained.[63] The absorption and emission spectra were recorded with a UV-Vis spectrometer (UV-2600, Shimadzu) and a spectrofluorophotometer (RF-5301PC, Shimadzu), respectively. All samples were excited at λ_{ex} = 350 nm. Dynamic light scattering (DLS) data were acquired using a laser light scattering spectrometer (Malvern Autosizer 4700) at 25 °C.

Preparation of star-shaped macroinitiator 21Br-β-CD based on β-CD (ref. 8)

β-CD (1.14 g, 1 mmol) was dissolved in 10 mL anhydrous 1-methyl-2-pyrrolidione and cooled to 0 °C. After that, 2-bromoisobutyryl bromide (9.6 mL, 42 mmol) was added dropwise to the β-CD solution under stirring. The resulting product was purified by washing sequentially with saturated $NaHCO_3$ aqueous solution (150 mL) and DI water (150 mL). The final product 21Br-β-CD was obtained by crystallizing in cold

n-hexane. The chemical structure of 21Br-β-CD was confirmed by ^{1}H-NMR in $CDCl_3$: $\delta = 1.8$ (broad s, 126H, CH_3), 3.5–5.4 (49H, sugar protons); FTIR: 2931 cm^{-1} (ν_{C-H}), 1737 cm^{-1} ($\nu_{C=O}$), 1158 cm^{-1} (ν_{C-O-C}), 1039 and 1105 cm^{-1} (coupled ν_{C-C} and ν_{C-O}).

Synthesis of 21-arm, star-shaped PS by ATRP using 21Br-β-CD as a macroinitiator

Polymerization of styrene (St) was performed using 21Br-β-CD as a star-shaped macroinitiator with 21 ATRP initiation sites. An ampoule charged with CuBr (0.0707 g), bpy (0.1539 g), 21Br-β-CD (0.1 g), and St (20 mL) was degassed by three freeze–pump–thaw cycles in liquid N_2, and then placed in an oil bath at 90 °C. The ampoules were taken out from the oil bath at different time intervals to stop the polymerization. The crude products were diluted by THF and passed through a neutral alumina column to remove the copper salt, and then precipitated in cold methanol. The products were purified by dissolution/precipitation with THF/cold methanol twice and then dried at 40 °C under vacuum. The whole process is outlined in Scheme 1.

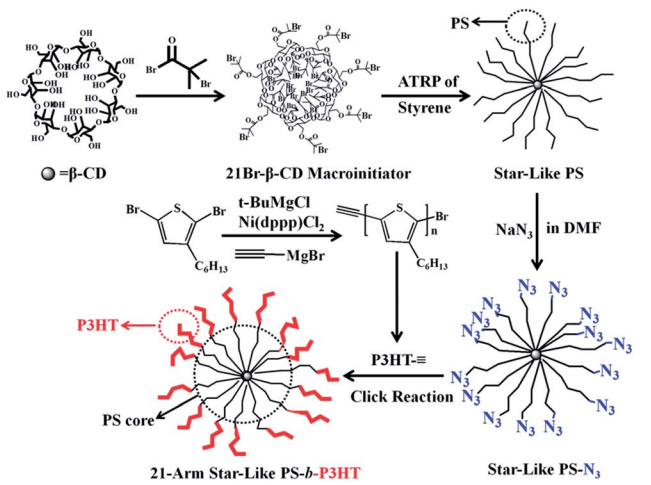

Scheme 1 Synthetic route to the 21-arm, star-shaped coil–rod PS-*b*-P3HT diblock copolymer.

Hydrolysis of star-shaped homopolymer PS for measuring the molecular weight of the PS arm

PS chains as arms in star-shaped PS were hydrolyzed under basic conditions:[64] 0.2 g star-shaped PS (sample-2 in Table 1) was dissolved in 50 mL THF; 10 mL KOH solution (1 M in ethanol) was then added. The mixture was refluxed for 72 h. After evaporation to dryness, the polymer was dissolved in chloroform and precipitated into acidified methanol. The products were purified twice by dissolution/precipitation with chloroform/methanol, and dried at 50 °C.

Synthesis of 21-arm, star-shaped azide-terminated PS (star-shaped PS-N_3)

Pure star-shaped PS-Br prepared by ATRP of styrene as noted above (1.0 g) was dissolved in DMF (10 mL), and sodium azide (Br in star-shaped PS : sodium azide = 1 : 10; molar ratio) was then added to the reaction solution. After the reaction for 24 h at room temperature, the excess NaN_3 was removed by centrifugation. The crude product was obtained by precipitating in cold methanol. It was then re-dissolved in chloroform (20 mL). The solution was washed with deionized water for three times. After that, the organic layer was dried by anhydrous $MgSO_4$, and the solution was precipitated in cold methanol. After filtration, the final product, 21-arm, star-shaped PS terminated with azide groups (*i.e.*, star-shaped PS-N_3), was dried at 40 °C in a vacuum oven for 4 h (yield = 86.5%). ^{1}H-NMR ($CDCl_3$, δ (ppm)): 6.33–7.31 (phenyl protons of PS), 1.21 (the methyl protons at the α-end of PS), 3.96 (the methine proton next to the end azide group on the PS), 2.50–1.22 (–CH_2CH(Ph)–, repeating units of PS backbone).

Synthesis of ethynyl-terminated P3HT (P3HT–≡)

A typical procedure for preparation of P3HT terminated with an ethynyl group is described as follow. 2,5-Dibromo-3-hexylthiophene (1.63 g, 5 mmol) was dissolved in anhydrous THF (10 mL) in a dry one-neck flask and stirred under Ar. *tert*-Butylmagnesium chloride (2.5 mL, 5 mmol) was injected using a syringe with a long needle. The reaction solution was stirred for

Table 1 Summary of the 21-arm, star-shaped PS homopolymer as an inner block

Entry	Time (h)	$M_{n,GPC}$[a]	M_w/M_n[b]	$M_{n,NMR}$[c]	$M_{n,theory}$[d]	$M_{n,PS}$[e]	E_T[f] (%)
Sample-1	2	76 100	1.14	142 440	133 200	6580	96.4
Sample-2	6	106 200	1.11	259 200	239 800	12 140	94.1
Sample-3	12	198 500	1.09	514 140	475 390	24 280	93.2

[a] Number-average molecular weight, $M_{n,GPC}$ determined by GPC, calibrated by linear PS standard. [b] Polydispersity index (PDI) measured by GPC. [c] Number-average molecular weight, $M_{n,NMR}$ calculated from ^{1}H-NMR data. [d] The theoretical values of M_n calculated from the monomer conversion and the concentration of initiators. [e] M_n of each PS arm calculated from ^{1}H-NMR data (Fig. S1) based on equation: $M_{n,PS} = \frac{\frac{A_b}{5}}{\frac{A_a}{6}} \times 104.15$ (1), where A_b and A_a are the integral area of phenyl protons on the PS chains and the integral area of methyl protons at the α-end of PS chains, respectively, and 104.15 is the molecular weight of the styrene (St) monomer. [f] The initiation efficiency of bromoisobutyryl for ATRP can be estimated from the ^{1}H-NMR spectra shown in Fig. S1, $E_T = \frac{M_{n,theory}}{21 \times M_{n,PS}} \times 100\%$ (2), where E_T is the reaction efficiency of bromoisobutyryl for ATRP, $M_{n,theory}$ is the theoretical M_n of star-shaped PS calculated from the monomer conversion and the concentration of the ATRP star-shaped macroinitiator 21Br-β-CD. $M_{n,PS}$ is the M_n of each PS arm calculated from the ^{1}H-NMR spectra.

2 h at room temperature. It was then diluted to 50 mL with anhydrous THF. Ni(dppp)Cl_2 (45 mg, 0.082 mmol) THF solution was added. The resulting reaction solution was first stirred for 10 min at room temperature, forming intermediate P3HT. Finally, the intermediate P3HT reacted with ethynylmagnesium bromide (4 mL, 2 mmol) in anhydrous THF for 30 min. The crude reaction solution was diluted by THF and passed through a neutral alumina column to remove the catalyst and magnesium salt, and then precipitated in cold methanol. The final pure product (ethynyl-terminated P3HT, *i.e.*, P3HT–≡) was purified by dissolution/precipitation with chloroform/cold methanol twice and then dried at 30 °C under vacuum (yield = 42.9%). The number-average molecular weights and PDI of ethynyl-terminated P3HT were 5600 g mol^{-1} (based on ^{1}H-NMR), 4800 g mol^{-1} (based on GPC) and 1.16 (GPC), respectively. ^{1}H-NMR ($CDCl_3$, δ (ppm)): $\delta = 6.98$ (s, 1H), $\delta = 3.50$ (s, 1H), $\delta = 2.8$ (t, 2H), $\delta = 1.7$ (m, 2H), $\delta = 1.43$ (m, 2H), $\delta = 1.36$ (m, 4H), and $\delta = 0.92$ (t, 3H).

Preparation of 21-arm, star-shaped diblock copolymers PS-*b*-P3HT by click reaction

Star-shaped PS-*b*-P3HT was synthesized *via* the click reaction of azide-terminated star-shaped PS with an excess of ethynyl-terminated P3HT. In a typical preparation, 21-arm, star-shaped PS-N_3 and P3HT–≡ were dissolved in toluene (10 mL) in an ampoule, and then CuBr and PMDETA were added. The reaction system (P3HT–≡ : star-shaped PS-N_3 : copper bromide : PMDETA = 1.2 : 1 : 10 : 10; molar ratio) was vacuumed by three freeze–pump–thaw cycles in liquid N_2. The ampoule was placed in an oil bath at 80 °C for 24 h. The crude product was diluted with chloroform and passed through an alumina column to remove the copper catalyst. The final product was precipitated in cold methanol and dried in a vacuum oven at 40 °C, yielding the 21-arm, star-shaped diblock copolymer, PS-*b*-P3HT.The whole process is outlined in Scheme 1.

Table 2 Summary of the 21-arm, star-shaped PS-*b*-P3HT diblock copolymer

Entry[a]	$M_{n,GPC}$[b]	M_w/M_n[c]	$M_{n,NMR}$[d]	Yield (%)	Efficiency[e] (%)
Sample-a	115 200	1.18	255 920	76.5	96.5
Sample-b	153 700	1.15	370 800	72.9	94.9
Sample-c	204 500	1.13	619 510	79.8	89.6

[a] Three samples (a, b, and c) were prepared by click reaction between P3HT–≡ and three star-shaped PS-N_3 from sample-1, sample-2, and sample-3 in Table 1, respectively. [b] Number-average molecular weight, $M_{n,GPC}$ determined by GPC, calibrated by linear PS standard. [c] The polydispersity index (DPI) determined by GPC. [d] Number-average molecular weight of star-shaped PS-*b*-P3HT, $M_{n,NMR}$ calculated from ^{1}H-NMR data: $M_{n,\text{star PS-}b\text{-P3HT}} = \frac{\frac{A_f}{2}}{\frac{(A_h - A_g)}{5}} \times \frac{M_{n,\text{star PS}}}{104.15} \times 166.3 + M_{n,\text{star PS}}$ (3), where A_f, A_g and A_h are the integral area of methene protons of the hexyl group on the P3HT block, the integral area of the protons on the thiophene ring of P3HT, and the integral area of phenyl protons on the PS chains, respectively, and 104.15 and 166.3 are the molecular weights of the St monomer and repeating unit of P3HT, respectively. $M_{n,\text{star PS}}$ is M_n of star-shaped PS (Table 1)calculated based on their ^{1}H-NMR spectra. [e] Efficiency of the click reaction ($E_{T\text{-Click}}$), calculated from ^{1}H-NMR spectra of the star-shaped PtBA-*b*-P3HT. Based on the ^{1}H-NMR spectrum of star-shaped PS-*b*-P3HT, the efficiency of the click reaction can be estimated by the following equation. $E_{T\text{-Click}} = \frac{\frac{A_f/2}{(A_h - A_g)/5} \times \frac{M_{n,\text{star PS}}}{104.15} \times 166.3}{21 \times M_{n,\text{P3HT}}} \times 100\%$ (4), where $E_{T\text{-Click}}$ is the reaction efficiency of the click reaction, and A_f, A_g and A_h are the integral area of methene protons of the hexyl group on the P3HT block, the integral area of the proton on the thiophene ring of P3HT, and the integral area of phenyl protons on the PS chains, respectively, and 104.15 and 166.3 are the molecular weights of the St monomer and repeating unit of P3HT, respectively. $M_{n,\text{star PS}}$ and $M_{n,\text{P3HT}}$ are M_n of star-shaped PS (Table 1) and of P3HT-ethynyl, respectively, calculated based on their ^{1}H-NMR spectra.

Fabrication of unimolecular micelles using star-shaped PS-*b*-P3HT

A small amount of the star-shaped PS-*b*-P3HT diblock copolymers (*i.e.*, ~1 mg; three samples in Table 2) were dissolved in anhydrous chloroform (~10 mL), a good solvent for both PS and P3HT blocks, at a concentration $c = 0.1$ mg mL^{-1} at room temperature. The resulting solution was stirred for 24 h.

Results and discussion

Preparation of 21-arm, star-shaped PS terminated with an azide end group (star-shaped PS-N_3)

As depicted in Scheme 1, the hydroxyl groups on β-cyclodextrin (β-CD) were esterified by 2-bromoisobutyryl bromide to form the star-shaped ATRP macroinitiator (*i.e.*, 21Br-β-CD).[8] Star-shaped homopolymer PS was synthesized by ATRP of styrene monomers in bulk at 90 °C, using 21Br-β-CD as a star-shaped macroinitiator, and bpy/CuBr as a catalyst. Three star-shaped PS samples with different molecular weights were synthesized as summarized in Table 1. Fig. 1 shows monomodal GPC traces for these three star-shaped PS samples. The molecular weight of star-shaped PS increased with low polydispersity index (PDI) (PDI < 1.15) as the polymerization time increased. Notably, the number-average molecular weight of star-shaped PS calculated based on the ^{1}H-NMR data was close to the theoretical values, but different from those obtained from GPC; this was resulted from the different

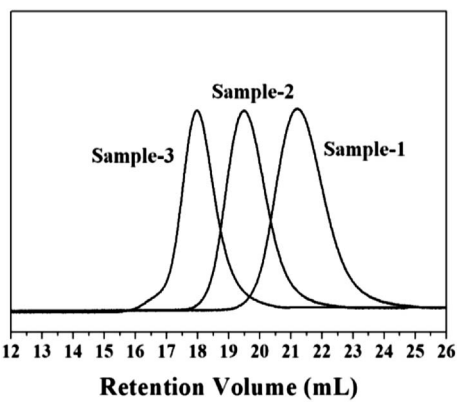

Fig. 1 GPC traces of 21-arm, star-shaped PS (*i.e.*, sample-1, sample-2, and sample-3 in Table 1).

hydrodynamic volume of star-shaped PS compared with the linear PS standard used in GPC measurements.

Fig. S1† shows the ^{1}H-NMR spectrum of star-shaped PS obtained by ATRP for 6 h (sample-2 in Table 1). A characteristic peak at $\delta = 6.33$–7.31 ppm (peak d) corresponded to the protons of phenyl rings of polystyrene chains. The peak at $\delta = 1.21$ ppm represented the methyl protons at the α-end of the PS arm. Subsequently, the bromine end groups on star-shaped PS were quantitatively transformed into azide groups through nucleophilic substitution reaction with NaN_3 in DMF. On the basis of the ^{1}H-NMR spectrum of 21-arm star-shaped PS-N_3, the conversion of –Br to –N_3 was confirmed as the peak corresponding to the methine protons next to the terminal bromine of PS-Br in Fig. S1† disappeared, and was replaced by a new peak at $\delta = 3.96$ ppm that belongs to the methine protons next to the end azide group on the PS arm. The successful conversion of –Br to –N_3 was further confirmed by the FTIR characterization, in which a characteristic stretching of –N_3 at 2112 cm^{-1} appeared (Fig. 2).

The initiation efficiency during ATRP of monomers has been widely investigated. It was well-known that not every initiating center generated a polymer arm and a non-100% initiation efficiency was attributed to steric hindrance from high density of initiating centers.[65–67] The density of initiating sites of 21Br-β-CD was much lower than that reported in the literature,[68] where 60–210 initiating sites were used in the ATRP process, thus higher initiation efficiency in this work is anticipated. The initiation efficiency during ATRP of styrene can be estimated based on the ^{1}H-NMR spectra, and the results are shown in Table 1. As expected, much higher E_T values for all three samples were obtained, suggesting that nearly all initiating sites of 21Br-β-CD took part in living radical polymerization of styrene monomers.

The number-average molecular weight of star-shaped PS obtained by GPC deviated from the real value because of the distinct difference in the hydrodynamic volume between the star-shaped PS and the linear PS standard. Thus, the detachment of PS arms from the β-CD core by hydrolyzing the ester group under the basic conditions followed by subsequent

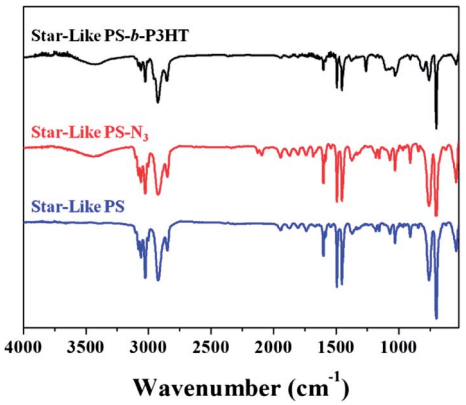

Fig. 2 FTIR spectra of 21-arm, star-shaped diblock copolymer PS-*b*-P3HT and its constituents. Star-shaped PS (sample-2 in Table 1; bottom blue curve), star-shaped PS-N_3 (middle red curve), and the corresponding star-shaped PS-*b*-P3HT (*i.e.*, sample-b in Table 2; top black curve).

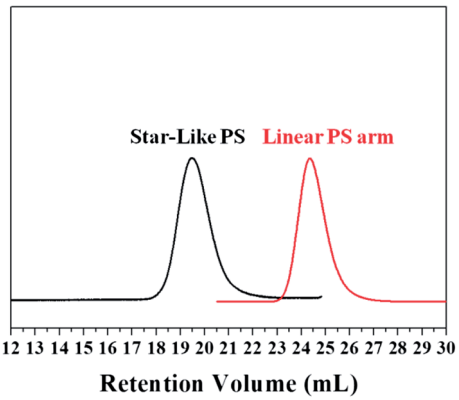

Fig. 3 GPC traces of star-shaped PS (sample-2 in Table 1) and the detached linear PS arm.

characterization of the molecular weight of the free linear PS arm was performed to offer the real number-average molecular weight of the PS arm (see the Experimental section). It is noteworthy that other star-shaped polymers (*e.g.*, poly(*tert*-butyl acrylate) (P*t*BA)) have been successfully synthesized in our previous studies.[8,35] However, as each repeat unit of these polymers contains the ester groups, when polymers are detached from the β-CD core by hydrolyzing the ester group at the α-end of polymer arms, the whole polymer chain would also be completely degraded. Thus, free polymer arms cannot be directly collected and characterized. In sharp contrast, in the current work, as PS arms possess no hydrolysable groups (*i.e.*, the ester group) under basic conditions, free linear PS arms detached from star-shaped PS can be readily obtained and characterized. Fig. 3 compares the GPC traces of the starting star-shaped PS and the detached PS arms. The monomodal peak with the narrow distribution (PDI = 1.12) was observed for the detached PS; the molecular weight of the PS arm, M_n was 13 010 g mol^{-1}, which is close to 12 140 g mol^{-1} derived from ^{1}H-NMR (the calculation of M_n of star-shaped PS was based on the hypothesis that all the initiating sites of 21Br-β-CD took part in initiating the polymerization of monomers). Thus, it also substantiated that the initiation efficiency of ATRP of styrene initiated by 21Br-β-CD was high.

Preparation of 21-arm, star-shaped diblock copolymers PS-*b*-P3HT by click reaction

The most popular click reaction is the copper-catalyzed Huisgen dipolar cycloaddition reaction between an azide and an alkyne that leads to the formation of 1,2,3-triazole.[69,70] In this work, a 21-arm, star-shaped PS-*b*-P3HT diblock copolymer was synthesized by click reaction between star-shaped PS-N_3 and P3HT terminated with an alkyne group (Scheme 1). P3HT–≡ was first synthesized by end-capping P3HT synthesized by the GRIM technique with ethynylmagnesium bromide.[71] The resulting star-shaped PS-*b*-P3HT diblock copolymers are summarized in Table 2. The successful coupling of 21-arm star-shaped PS-N_3 with P3HT–≡ to yield 21-arm star-shaped PS-*b*-P3HT diblock copolymers was also verified by ^{1}H-NMR, FTIR and GPC as

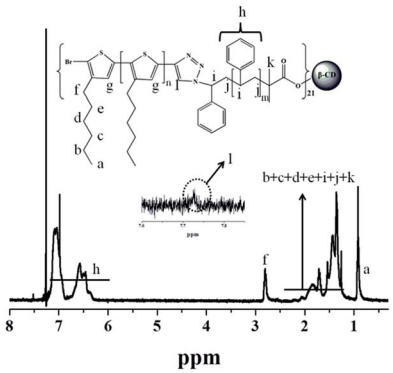

Fig. 4 ^{1}H-NMR spectrum of 21-arm, star-shaped PS-*b*-P3HT (*i.e.*, sample-b in Table 2; solvent: $CDCl_3$).

discussed in the following. Fig. 4 shows the ^{1}H-NMR spectrum of star-shaped PS-*b*-P3HT. All resonance signals from the PS and P3HT blocks are clearly discernible. Compared to the ^{1}H-NMR spectrum of star-shaped PS-N_3, the characteristic peak of $-CH_2CH(Ph)-N_3$ (*i.e.*, the end group of the PS block) disappeared in the star-shaped PS-*b*-P3HT diblock copolymer. At the same time, a signal associated with the triazole ring at δ = 7.72 ppm appeared (peak l). The characteristic peaks at δ = 6.33–7.31 ppm (peak h) from the protons of phenyl rings in PS chains and at δ = 0.92–2.80 ppm from the hexyl group in P3HT confirmed the success in coupling star-shaped PS-N_3 with P3HT–≡. In addition, based on the ^{1}H-NMR spectrum of star-shaped PS-*b*-P3HT, the efficiency ($E_{T\text{-}Click}$) of click reaction can be calculated from eqn (4) in the note of Table 2. High $E_{T\text{-}Click}$ were found (in Table 2), indicating that almost all coupling sites in star-shaped PS-N_3 were reacted with P3HT–≡. Moreover, compared to two constituents (*i.e.*, star-shaped PS-N_3 and linear P3HT–≡), the FTIR spectral change in the star-shaped PS-*b*-P3HT diblock copolymer also supported the complete click coupling as the characteristic stretching of $-N_3$ at 2112 cm^{-1} was no longer observable (Fig. 2).

Fig. 5 compares the GPC traces of the final product 21-arm, star-shaped PS-*b*-P3HT with its two constituents. All samples had a nearly monomodal GPC traces and a narrow PDI (<1.2).

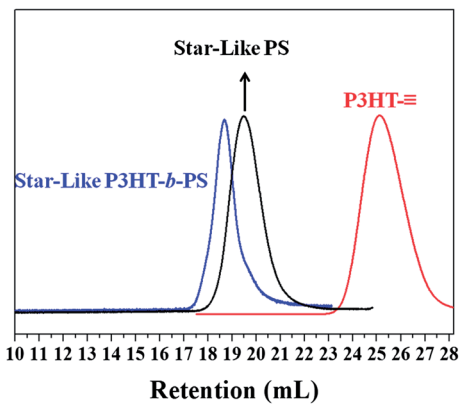

Fig. 5 GPC traces of 21-arm, star-shaped PS-*b*-P3HT (*i.e.*, sample-b in Table 2) and the corresponding star-shaped PS (*i.e.*, sample-2 in Table 1) and linear P3HT–≡.

Similarly, the molecular weights of star-shaped PS-*b*-P3HT measured by GPC deviated from those calculated from ^{1}H-NMR data. This is due to the different hydrodynamic volume of star-shaped diblock copolymers compared to the linear PS standard in GPC characterization (Table 2). In order to ensure each PS-N_3 arm to couple with linear P3HT–≡, the excess amount of P3HT–≡ was added into the reaction system (20% excess as compared to the PS-N_3 arm; molar ratio). After coupling reaction, the excess amount of P3HT–≡ was easily removed by fractional precipitation using chloroform as the solvent and cold methanol as the precipitator as the final product had much larger molecular weight than linear P3HT–≡.

Absorption and photoluminescence (PL) of multi-arm star-shaped PS-*b*-P3HT

The UV-Vis absorption and photoluminescence (PL) spectra of star-shaped PS-*b*-P3HT (sample-b in Table 2), star-shaped PS-N_3, and linear P3HT–≡ in solution are shown in Fig. 6. Clearly, the absorption spectrum of star-shaped PS-*b*-P3HT was the sum of the spectral features from its two constituents (Fig. 6A), that is, the absorption of phenyl rings in PS arms below 300 nm from star-shaped PS-N_3 and the absorption of thiophene in the P3HT block above 400 nm from P3HT–≡, which served as additional evidence of successful click coupling of star-shaped PS-N_3 and linear P3HT–≡. The same absorption maxima at around 448 nm were observed for both P3HT–≡ and star-shaped PS-*b*-P3HT block copolymer chloroform solutions. The photoluminescence (PL) spectra of star-shaped PS-*b*-P3HT and the two corresponding constituents are shown in Fig. 6B. Notably, the star-shaped PS-*b*-P3HT block copolymer displayed very similar

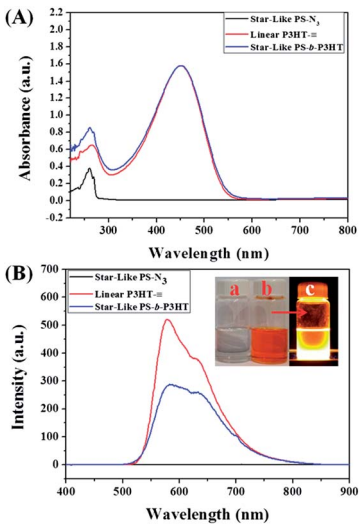

Fig. 6 (A) Absorption spectra of star-shaped PS-N_3 (from sample-2 in Table 1, black line), linear P3HT–≡ (red line), and star-shaped PS-*b*-P3HT (sample-b in Table 2, blue line). (B) Emission spectra of star-shaped PS-N_3 (from sample-2 in Table 1, black line), linear P3HT–≡ (red line), and star-shaped PS-*b*-P3HT (sample-b in Table 2, blue line). All the samples were dissolved in chloroform at the concentration c = 0.1 mg mL^{-1}. Digital images of (a) star-shaped PS-N_3, (b and c) star-shaped PS-*b*-P3HT before (b) and after (c; emitting red fluorescence) UV illumination are shown as insets.

emission peaks with P3HT–≡, while star-shaped PS-N_3 had no emission. The 21-arm star-shaped PS-*b*-P3HT emitted red fluorescence under UV illumination (the inset in Fig. 6B). In addition, compared with linear P3HT–≡, the emission intensity of star-shaped PS-*b*-P3HT decreased due to the introduction of PS blocks that reduced the percentage of P3HT blocks in the solution while the concentration of all samples used in the PL measurements was kept the same. The optical properties noted above further proved that the P3HT blocks were successfully introduced to yield star-shaped coil–rod diblock copolymers.

Unimolecular micelles of multi-arm, star-shaped PS-*b*-P3HT

Different from conventional micelles formed from the self-assembly of linear block copolymers, the unimolecular micellar structures intrinsically yielded from 21-arm star-shaped PS-*b*-P3HT diblock copolymers are static rather than dynamic. These structures can form uniform and structurally stable spherical unimolecular micelles.[72–74] Compared to other PAA-based star-shaped amphiphilic copolymers previously reported by us,[8,35] as both PS and P3HT blocks are hydrophobic, the star-shaped PS-*b*-P3HT can be readily dissolved into a large variety of organic solvents (*e.g.*, toluene, THF, chloroform, *etc.*). In this work, the star-shaped PS-*b*-P3HT block copolymers were completely dissolved in chloroform, a good solvent for both PS and P3HT blocks, thereby leading to the formation of unimolecular micelles (concentration, $c = 0.1$ mg mL^{-1}). The hydrodynamic diameter $D_h \sim 15$ nm (Table S1†) of unimolecular micelles produced by star-shaped PS-N_3 (from sample-2 in Table 1) was measured by DLS. After the outer P3HT blocks were introduced into star-shaped polymers by coupling reaction, D_h increased to ~26 nm (Table S1†). They possessed uniform size distribution as evidenced by the DLS characterization with a narrow peak (Fig. S2†). With the increase in the molecular weights of star-shaped PS-N_3 and the corresponding star-shaped PS-*b*-P3HT, the average diameter of unimolecular micelles of star-shaped PS-N_3 increased from ~10 nm (from sample-a in Table 1) to ~22 nm (from sample-3 in Table 1). At the same time, the average diameter of unimolecular micelles of star-shaped PS-*b*-P3HT also increased from ~18 nm (sample-a in Table 2) to ~31 nm (sample-c in Table 2) according to the DLS studies (Table S1†).

AFM characterizations were also performed to reveal the morphologies of unimolecular micelles. The chloroform solution of star-shaped PS-N_3 (from sample-2 in Table 1) and the resulting star-shaped PS-*b*-P3HT (*i.e.*, sample-b in Table 2) were spin-coated on the Si substrate. Clearly, both star-shaped PS-N_3 and star-shaped PS-*b*-P3H formed spherical unimolecular micelles with an average diameter of ~18 nm (Fig. 7A and B) and ~29 nm (Fig. 7C and D), and an average height of ~12 nm (Fig. 7A) and ~19 nm (Fig. 7C), respectively, in accordance with $D_h \sim 15$ nm and ~26 nm in the DLS measurements. We note that D_h values obtained from DLS were smaller than those from AFM, and moreover the heights of micelles obtained by AFM were smaller than their diameters; this may be reasonable as regular spherical micelles collapsed and adopted an extended flat-on conformation after spin-coating the star-shaped PS-*b*-P3HT chloroform solution on the Si substrate.[75] In addition,

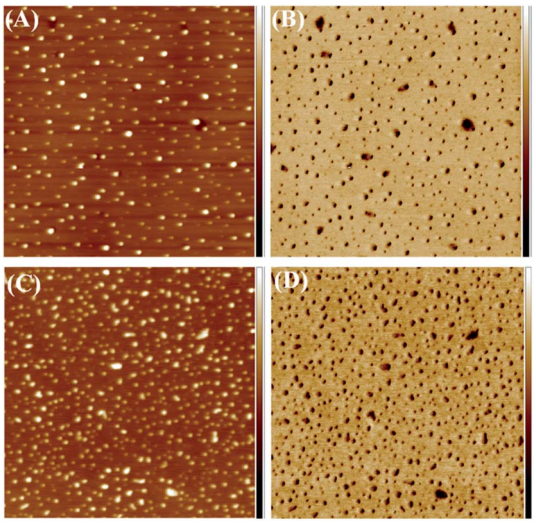

Fig. 7 AFM images of star-shaped PS-N_3 and the corresponding star-shaped PS-*b*-P3HT. (A) AFM height and (B) phase images of star-shaped PS-N_3 (from sample-2 in Table 1). Image size = 2.5 × 2.5 μm^2, and *Z* range = 17 nm for (A) and 55° for (B). (C) AFM height and (D) phase images of star-shaped PS-*b*-P3HT (sample-b in Table 2). Image size = 2.5 × 2.5 μm^2, and *Z* range = 15 nm for (C) and 86° for (D).

during the AFM measurements, the tip-broadening effect may arise artifactual broadening of measured unimolecular micelles; this also led to a larger size of micelles and the formation of an extended flat-on conformation.[76] In addition to the majority of uniform but smaller particle-shaped nanostructures, some irregular yet larger ones were also seen. These larger particle-shaped nanostructures may be formed due to the aggregation of several adjacent unimolecular micelles due to the weak affinity of PS and P3HT on the SiO_2-coated Si substrate during the spin-coating process.[77] To further explore the morphology of star-shaped PS-N_3 and the resulting star-shaped PS-*b*-P3HT unimolecular micelles, TEM imaging was conducted. The dark dots in the TEM micrographs corresponded to the star-shaped PS-N_3 (diameter: ~16 nm) and the resulting star-shaped PS-*b*-P3HT (diameter: ~28 nm) as RuO_4 stained both PS and P3HT blocks.[63] The sizes of two samples are in good accordance with the results measured by DLS and AFM.

Conclusions

In summary, by combining living polymerization with click reaction, star-shaped coil–rod PS-*b*-P3HT diblock copolymers composed of well-defined inner coil-shaped PS blocks and outer rod-shaped P3HT blocks were synthesized. These star-shaped diblock copolymers possessed narrow molecular weight distribution, and the molecular weight of PS and P3HT blocks can be precisely controlled by varying the polymerization conditions during ATRP and quasi-living GRIM, respectively. The success of coupling of azide-functionalized PS and ethynyl-terminated P3HT to yield star-shaped PS-*b*-P3HT was substantiated by GPC, ^{1}H NMR, FTIR, UV-Vis, and photoluminescence measurements. The absorption and emission spectra of star-shaped PS-*b*-P3HT were the sum of two constituents (*i.e.*, azide-functionalized PS

and ethynyl-terminated P3HT). These star-shaped PS-*b*-P3HT formed unimolecular micelles in good solvent. The ability to prepare star-shaped coil–rod block copolymers with well controlled molecular architecture (*i.e.*, arm structures and compositions) and molecular weights offers the opportunity for exploring their structure (*i.e.*, star-shaped architecture and the coil–rod conformation) and property relationship for potential applications in optoelectronics, biosensors, *etc.*

Acknowledgements

We gratefully acknowledge funding support from the Air Force Office of Scientific Research (FA9550-13-1-0101) and Key Laboratory of Computational Physical Sciences at Fudan University.

Notes and references

1 A. Guo, G. Liu and J. Tao, *Macromolecules*, 1996, **29**, 2487–2493.
2 H. Gao and K. Matyjaszewski, *Macromolecules*, 2006, **39**, 4960–4965.
3 N. Hadjichristidis, M. Pitsikalis, S. Pispas and H. Iatrou, *Chem. Rev.*, 2001, **101**, 3747–3792.
4 E. R. Zubarev, R. V. Talroze, T. I. Yuranova, N. A. Plate and H. Finkelmann, *Macromolecules*, 1998, **31**, 3566–3570.
5 T. H. Mourey, S. R. Turner, M. Rubinstein, J. M. J. Frechet, C. J. Hawker and K. L. Wooley, *Macromolecules*, 1992, **25**, 2401–2406.
6 C. J. Hawker, P. J. Farrington, M. E. Mackay, K. L. Wooley and J. M. J. Frechet, *J. Am. Chem. Soc.*, 1995, **117**, 4409–4410.
7 J. F. G. A. Jansen, E. M. M. de Brabander-van den Berg and E. W. Meijer, *Science*, 1994, **266**, 1226–1229.
8 X. Pang, L. Zhao, M. Akinc, J. K. Kim and Z. Lin, *Macromolecules*, 2011, **44**, 3746–3752.
9 K. Hatada, T. Nishiura, T. Kitayama and K. Ute, *Macromol. Symp.*, 1997, **118**, 135–141.
10 D. T. Wu, *Synth. Met.*, 2002, **126**, 289–293.
11 K. Char, C. W. Frank and A. P. Gast, *Langmuir*, 1989, **5**, 1335–1340.
12 K. Char, C. W. Frank and A. P. Gast, *Langmuir*, 1989, **5**, 1096–1105.
13 K. Char, C. W. Frank and A. P. Gast, *Macromolecules*, 1989, **22**, 3177–3180.
14 C. Barner-Kowollik, P. Vana, J. F. Quinn and T. P. Davis, *J. Polym. Sci., Part A: Polym. Chem.*, 2002, **40**, 1058–1063.
15 S. C. Farmer and T. E. Patten, *J. Polym. Sci., Part A: Polym. Chem.*, 2002, **40**, 555–563.
16 C. J. Hawker, *Angew. Chem., Int. Ed.*, 1995, **34**, 1456–1459.
17 J. Filley, J. T. McKinnon, D. T. Wu and G. H. Ko, *Macromolecules*, 2002, **35**, 3731–3738.
18 Y. J. Gong, Z. H. Li, D. Wu, Y. H. Sun, F. Deng, Q. Luo and Y. Yue, *J. Mater. Res.*, 2002, **17**, 431–437.
19 Y. J. Gong, Z. H. Li, D. Wu, Y. H. Sun, F. Deng, Q. Luo and Y. Yue, *Acta Phys.-Chim. Sin.*, 2002, **18**, 572–576.
20 Y. J. Gong, D. Wu and Y. H. Sun, *Prog. Chem.*, 2002, **14**, 1–7.
21 Y. H. Kim, W. T. Ford and T. H. Mourey, *J. Polym. Sci., Part A: Polym. Chem.*, 2007, **45**, 4623–4634.
22 K. L. Genson, J. Hoffman, J. Teng, E. R. Zubarev, D. Vaknin and V. V. Tsukruk, *Langmuir*, 2004, **20**, 9044–9052.
23 J. Teng and E. R. Zubarev, *J. Am. Chem. Soc.*, 2003, **125**, 11840–11841.
24 R. T. A. Mayadunne, J. Jeffery, G. Moad and E. Rizzardo, *Macromolecules*, 2003, **36**, 1505–1513.
25 K. Inoue, *Prog. Polym. Sci.*, 2000, **25**, 453–571.
26 K. Matyjaszewski, P. J. Miller, J. Pyun, G. Kickelbick and S. Diamanti, *Macromolecules*, 1999, **32**, 6526–6535.
27 Q. Wei, T. Nishizawa, K. Tajima and K. Hashimoto, *Adv. Mater.*, 2008, **20**, 2211–2216.
28 L. Zhao and Z. Lin, *Adv. Mater.*, 2012, **24**, 4353–4368.
29 M. He, F. Qiu and Z. Lin, *J. Mater. Chem.*, 2011, **21**, 17039–17048.
30 M. Byun, R. L. Laskowski, M. He, F. Qiu, M. Jeffries-El and Z. Lin, *Soft Matter*, 2009, **5**, 1583–1586.
31 J. Xu, J. Wang, M. Mitchell, P. Mukherjee, M. Jeffries-El, J. W. Petrich and Z. Lin, *J. Am. Chem. Soc.*, 2007, **129**, 12828–12833.
32 R. D. McCullough, *Adv. Mater.*, 1998, **10**, 93–116.
33 B. C. Thompson and J. M. J. Fréchet, *Angew. Chem., Int. Ed.*, 2008, **47**, 58–77.
34 M. Jeffries-El, G. Sauvé and R. D. McCullough, *Macromolecules*, 2005, **38**, 10346–10352.
35 X. Pang, L. Zhao, C. Feng and Z. Lin, *Macromolecules*, 2011, **44**, 7176–7183.
36 J. S. Liu, E. Sheina, T. Kowalewski and R. D. McCullough, *Angew. Chem., Int. Ed.*, 2001, **41**, 329–332.
37 M. C. Iovu, M. Jeffries-El, E. E. Sheina, J. R. Cooper and R. D. McCullough, *Polymer*, 2005, **46**, 8582–8586.
38 M. C. Iovu, R. Zhang, J. R. Cooper, D. M. Smilgies, A. E. Javier, E. E. Sheina, T. Kowalewski and R. D. McCullough, *Macromol. Rapid Commun.*, 2007, **28**, 1816–1824.
39 C. A. Dai, W. C. Yen, Y. H. Lee, C. C. Ho and W. F. Su, *J. Am. Chem. Soc.*, 2007, **129**, 11036–11038.
40 R. Gunawidjaja, Y. N. Luponosov, F. F. Huang, S. A. Ponomarenko, A. M. Muzafarov and V. V. Tsukruk, *Langmuir*, 2009, **25**, 9270–9284.
41 M. G. Alemseghed, S. Gowrisanker, J. Servello and M. C. Stefan, *Macromol. Chem. Phys.*, 2009, **210**, 2007–2014.
42 M. G. Alemseghed, J. Servello, N. Hundt, P. Sista, M. C. Biewer and M. C. Stefan, *Macromol. Chem. Phys.*, 2010, **211**, 1291–1297.
43 B. W. Boudouris, C. D. Frisbie and M. A. Hillmyer, *Macromolecules*, 2008, **41**, 67–75.
44 M. He, L. Zhao, J. Wang, W. Han, Y. L. Yang, F. Qiu and Z. Q. Lin, *ACS Nano*, 2010, **4**, 3241.
45 P. T. Wu, G. Q. Ren, C. X. Li, R. Mezzenga and S. A. Jenekhe, *Macromolecules*, 2009, **42**, 2317.
46 W. Han, M. He, M. Byun, B. Li and Z. Lin, *Angew. Chem., Int. Ed.*, 2013, **52**, 2564–2568.
47 B. J. de Gans, S. Wiegand, E. R. Zubarev and I. Stupp, *J. Phys. Chem. B*, 2002, **106**, 9730–9736.
48 A. Takahashi, Y. Rho, T. Higashihara, B. Ahn, M. Ree and M. Ueda, *Macromolecules*, 2010, **43**, 4843–4852.

49 C. P. Radano, O. A. Scherman, N. Stingelin-Stutzmann, C. Müller, D. W. Breiby, P. Smith, R. A. J. Janssen and E. W. Meijer, *J. Am. Chem. Soc.*, 2005, **127**, 12502–12503.
50 C.-A. Dai, W.-C. Yen, Y.-H. Lee, C.-C. Ho and W.-F. Su, *J. Am. Chem. Soc.*, 2007, **129**, 11036–11038.
51 B. Li, G. Sauvé, M. C. Iovu, M. Jeffries-El, R. Zhang, J. Cooper, S. Santhanam, L. Schultz, J. C. Revelli, A. G. Kusne, T. Kowalewski, J. L. Snyder, L. E. Weiss, G. K. Fedder, R. D. McCullough and D. N. Lambeth, *Nano Lett.*, 2006, **6**, 1598–1602.
52 G. Sauvé and R. D. McCullough, *Adv. Mater.*, 2007, **19**, 1822–1825.
53 V. Coessens, T. Pintauer and K. Matyjaszewski, *Prog. Polym. Sci.*, 2001, **26**, 337–377.
54 H. C. Kolb, M. G. Finn and K. B. Sharpless, *Angew. Chem., Int. Ed.*, 2001, **40**, 2004–2021.
55 W. H. Binder and R. Sachsenhofer, *Macromol. Rapid Commun.*, 2007, **28**, 15–54.
56 X. Luo, G. Wang, X. Pang and J. Huang, *Macromolecules*, 2008, **41**, 2315–2317.
57 K. Ohno, B. Wong and D. M. Haddleton, *J. Polym. Sci., Part A: Polym. Chem.*, 2001, **39**, 2206–2214.
58 K. Matyjaszewski, S. G. Gaynor, A. Kulfan and M. Podwika, *Macromolecules*, 1997, **30**, 5192–5194.
59 W. H. Yu, E. T. Kang, K. G. Neoh and S. P. Zhu, *J. Phys. Chem. B*, 2003, **107**, 10198–10205.
60 K. Huang and J. Rzayev, *J. Am. Chem. Soc.*, 2009, **131**, 6880–6885.
61 L. Zhao, X. Pang, R. Adhikary, J. W. Petrich, M. Jeffries-El and Z. Lin, *Adv. Mater.*, 2011, **23**, 2844–2849.
62 L. Zhao, X. Pang, R. Adhikary, J. W. Petrich and Z. Lin, *Angew. Chem., Int. Ed.*, 2011, **123**, 4044–4048.
63 X. Wang, W. H. Lee, G. Zhang, X. Wang, B. Kang, H. Lu, L. Qiu and K. Cho, *J. Mater. Chem. C*, 2013, **1**, 3989–3998.
64 G. Cheng, A. Böker, M. Zhang, G. Krausch and A. H. E. Müller, *Macromolecules*, 2001, **34**, 6883–6888.
65 D. Neugebauer, B. S. Sumerlin, K. Matyjaszewski, B. Goodhart and S. S. Sheiko, *Polymer*, 2004, **45**, 8173–8179.
66 B. S. Sumerlin, D. Neugebauer and K. Matyjaszewski, *Macromolecules*, 2005, **38**, 702–708.
67 F. A. Plamper, H. Becker, M. Lanzendörfer, M. Patel, A. Wittemann, M. Ballauff and A. H. E. Müller, *Macromol. Chem. Phys.*, 2005, **206**, 1813–1825.
68 C. Liu, G. W. Wang, Y. Zhang and J. L. Huang, *J. Appl. Polym. Sci.*, 2008, **108**, 777–784.
69 V. V. Rostovtsev, L. G. Green, V. V. Fokin and K. B. Sharpless, *Angew. Chem., Int. Ed.*, 2002, **41**, 2596–2599.
70 C. W. Tornøe, C. Christensen and M. Meldal, *J. Org. Chem.*, 2002, **67**, 3057–3064.
71 M. Jeffries-El, G. Sauve and R. D. McCullough, *Macromolecules*, 2005, **38**, 10346–10352.
72 A. W. Bosman, H. M. Janssen and E. W. Meijer, *Chem. Rev.*, 1999, **99**, 1665–1688.
73 S. E. Stiriba, H. Frey and R. Haag, *Angew. Chem., Int. Ed.*, 2002, **41**, 1329–1334.
74 P. Veprek and J. Jezek, *J. Pept. Sci.*, 1999, **5**, 203–220.
75 M. Ornatska, S. Peleshanko, K. L. Genson, B. Rybak, K. N. Bergman and V. V. Tsukruk, *J. Am. Chem. Soc.*, 2004, **126**, 9675–9684.
76 K. Meinander, T. N. Jensen, S. B. Simonsen, S. Helveg and J. V. Lauritsen, *Nanotechnology*, 2012, **23**, 405705.
77 S. W. Hong, J. Wang and Z. Lin, *Angew. Chem., Int. Ed.*, 2009, **48**, 8356–8360.